DOI: 10.1002/adma.200601608

High-Performance Organic Semiconductors Based on Fluorene–Phenylene Oligomers with High Ionization Potentials**

By *Jason Locklin*, *Mang Mang Ling*, *Andrew Sung*, *Mark E. Roberts*, and *Zhenan Bao**

While mobility values in organic field-effect transistors (OFETs) continue to rise with the optimization of molecular structures, morphological improvements, and device architectures, operational stability under ambient conditions still remains a major issue. Most of the high-performance p-channel semiconductors, such as fused-ring acenes, oligothiophenes, and their derivatives have high-energy oxidation potentials that lead to photochemical instabilities and degradation of device performance when operated in the presence of oxygen and moisture.[1,2] The exact mechanism of this degradation is not completely understood, but previous work has proposed the formation of traps at, or interaction with, grain boundaries, which can reduce the on-current, shift the threshold voltage, or increase the off-current in the device.[3,4] Recent work points to a plausible mechanism that involves photoinduced doping, which has been observed in both oligomeric and polymeric derivatives.[5] Degradation by thermal and photo-oxidation has also been proposed in pentacene devices.[6]

Recently, synthetic design has been used to increase the ionization potential of the organic semiconductor both sterically, by reducing π-orbital overlap between adjacent rings, and electronically, which has been demonstrated with both oligomeric materials and polymers.[7–10] Typically, this has been detrimental to the field-effect mobility, and in the select cases where mobilities higher than 0.1 $cm^2\,V^{-1}\,s^{-1}$ have been observed, high substrate deposition temperatures (T_Ds) were used, which can limit integration with plastic substrates. For example, sexiphenylene (6P), with a very high ionization potential (–6.1 eV),[11] had a mobility of only 0.07 $cm^2\,V^{-1}\,s^{-1}$ when deposited at $T_D = 200\,°C$.[12] Typically, at least one or two thiophene units are incorporated into the oligomer to lower the ionization energy and mobilities greater than 0.1 $cm^2\,V^{-1}\,s^{-1}$ can be achieved with such oligomers.[7,8] It should be noted that Meng et al. recently obtained a mobility of 0.5 $cm^2\,V^{-1}\,s^{-1}$ in a stable thiophene–anthracene co-oligomer by using a two-stage deposition process at 120 and 80 °C.[13]

In this report, we describe the synthesis and device performance of three fluorene–phenylene co-oligomers with very high ionization potentials that show high device performance with excellent chemical stability. Average field-effect mobilities as high as 0.32 $cm^2\,V^{-1}\,s^{-1}$ and on/off ratios of ca. 10^8 have been achieved with devices deposited onto octadecyltrimethoxysilane (OTS) treated substrates held at temperatures of 50 °C when measured under ambient conditions. This is the highest mobility value reported for oligomers with ionization potentials higher than –5.5 eV.

Figure 1 shows the molecular structures of the fluorene–phenylene derivatives used in this study. The semiconductors were synthesized using Suzuki coupling between the pinacolato boronic ester or boronic acid and the corresponding dibrominated core. All derivatives are relatively insoluble in common organic solvents, and were purified twice by gradient sublimation under vacuum. Each oligomer was collected as an off-white powder. The final products were verified by mass spectrometry and elemental analysis. The thermal stability of each oligomer was investigated using thermogravimetric analysis (TGA), where no decomposition was observed up to 435 °C under N_2.

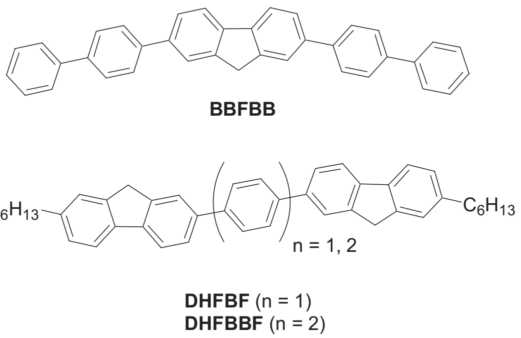

Figure 1. Chemical structures of phenylene–fluorene co-oligomers used in this study.

Table 1 shows the electrochemical data obtained from cyclic voltammetry. The experiments were performed under argon in a saturated solution of anhydrous methylene chloride with 0.1 M tetrabutylammonium hexafluorophosphate (Bu_4NPF_6) as the supporting electrolyte, at a scan rate of 50 $mV\,s^{-1}$. For all oligomers, one quasireversible oxidation

---

[*] Prof. Z. Bao, Dr. J. Locklin, Dr. M. M. Ling, A. Sung, M. E. Roberts
Department of Chemical Engineering, Stanford University
Stanford, CA 94305-5025 (USA)
E-mail: zbao@stanford.edu

[**] JL thanks the Intelligence Community Postdoctoral Fellowship for financial support. ZB acknowledges partial financial support from the Finmeccanica Faculty Scholar Award, the 3M Faculty Award, the Center for Polymeric Interfaces and Macromolecular Assemblies (NSF-Center MRSEC under Award Number DMR-0213618). Supporting Information is available online from Wiley InterScience or from the author.

Table 1. Electrochemical data for the phenylene–fluorene oligomers. [a]

Oligomer	E_{pc}/E_{pa} [V] [b]	$E_{1/2}$ [V] [c]	HOMO [eV]
BBFBB	0.92/0.83	0.88	–5.68
DHFBF	0.84/0.69	0.77	–5.57
DHFBBF	0.80/0.70	0.77	–5.57

[a] CH_2Cl_2, scan rate: 50 mV s^{-1}, Ag pseudoreference. All potentials are reported vs. the Fc/Fc^+ redox couple (0.598 V in this system). [b] Peak potentials of cathodic (E_{pc}) and anodic (E_{pa}) peaks. [c] $E_{1/2}$: formal potential.

wave was observed within the range of the solvent and electrolyte window. The results are shown in Table 1. No reduction waves were observed for any of the oligomers. For each oligomer, the highest occupied molecular orbital (HOMO) level was estimated using the formal potential ($E_{1/2}$) with the assumption that ferrocene, used as the internal standard, has a HOMO level of –4.8 eV.[14] For DHFBF and DHFBBF, one partially reversible oxidation wave was observed with an $E_{1/2}$ of 0.77 V versus the ferrocene/ferrocenium redox couple as an internal standard. This corresponds to a HOMO level of approximately –5.57 eV. This is 0.21 eV lower than reported in the corresponding fluorene–bithiophene oligomer under the same conditions[9] and slightly higher than the corresponding all-phenylene derivative with the same number of rings (6P, –6.1 eV). The optical bandgap for DHFBBF, determined from a thin film deposited on glass, is 3.02 eV.

Thin films of the purified oligomers were deposited onto SiO_2 (300 nm)/n-doped Si substrates, which had been modified using a self-assembled monolayer of OTS (contact angle >95°). OFETs were completed by depositing gold electrodes through a shadow mask. Out-of-plane X-ray diffraction of the films shows high crystallinity (Fig. 2b and Supporting Information). With DHFBBF, multiple (00*l*) reflections are observed from a film 40 nm in thickness ($T_D = 50$ /C), with an estimated molecular length of ca. 38 Å after energy minimization ($d1 = 37.6$ Å, $d2 = 18.6$ Å, $d3 = 12.5$ Å, $d4 = 9.3$ Å, $d5 = 7.5$ Å, $d6 = 6.2$ Å, $d7 = 4.7$ Å, $d8 = 3.8$ Å). These spacings are consistent with the monomolecular layer thickness obtained by atomic force microscopy (AFM), as shown below, which indicate near-perpendicular alignment of the molecules with respect to the substrate surface. X-ray analysis of BBFBB also shows high crystallinity, but with multiple crystalline phases apparent ($d = 13.3$, 10.6, 8.9, 6.7, 5.3, 4.6, 4.4, 4.0 Å). The energy-minimized molecular length was estimated to be ca. 25 Å. This molecule cannot be completely linear, due to the 2,7 linkage of the central fluorene moiety.

Tapping-mode AFM of a film consisting of ca. 5 nm of DHFBBF deposited at a substrate temperature of 50 °C is shown in Figure 2a (5 µm × 5 µm). The film consists of an almost continuous first molecular layer, with few grain boundaries. The height of the second layer (ca. 3.8 nm) is consistent with the *d*-spacing obtained from X-ray measurements. Both the alkyl chains on the molecule, which lead to a decrease in both substrate–molecule and interlayer interactions, and the long aspect ratio favor the 2D layer-by-layer growth, which is optimal for high charge-carrier mobility in thin-film devices.[15–17]

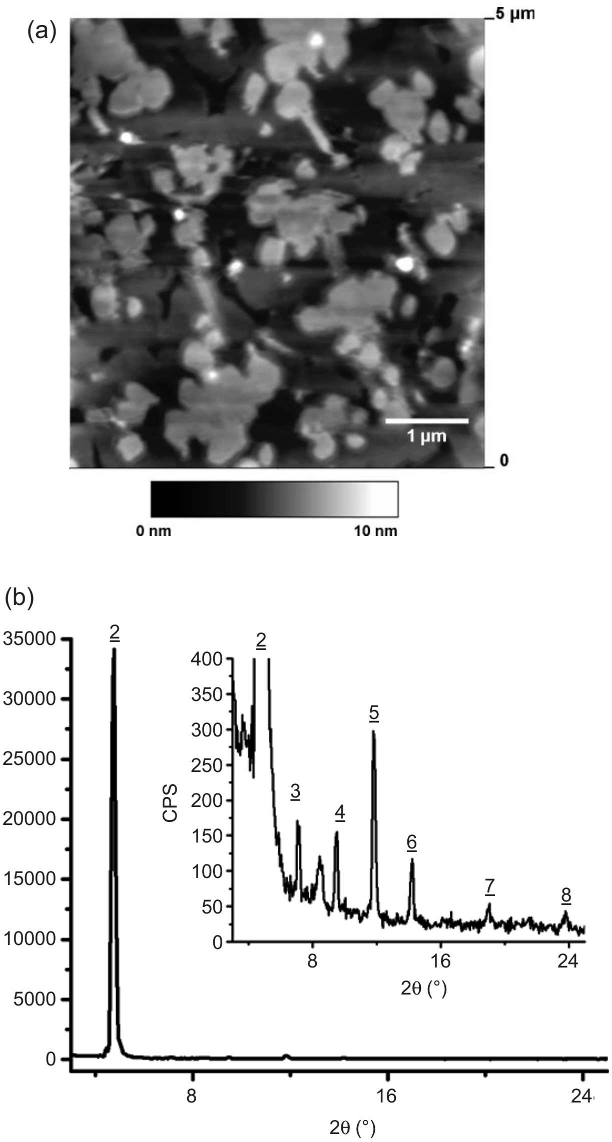

Figure 2. a) Atomic force microscopy (AFM) topography image (5 µm × 5 µm) of a ca. 5 nm thick film of DHFBBF deposited at $T_D = 50$ °C. The surface coverage consists of ca. 1.5 monolayers (ML). The first molecular layer consists of a continuous granular morphology. b) Out-of-plane X-ray diffraction of a 40 nm film of DHFBBF deposited at $T_D = 50$ °C. The inset is magnified 10×.

Table 2 lists the semiconductor device parameters for each oligomer. All oligomers show well-defined linear and saturation-regime output characteristics (see Supporting Information). The threshold voltage is relatively large, due to the large energy level mismatch between the oligomers and the Fermi level of the Au electrodes. The mobility of DHFBBF is much greater than the other oligomers, reaching an average of 0.32 $cm^2 V^{-1} s^{-1}$ at $T_D = 50$ °C. The highest value we obtained was 0.45 $cm^2 V^{-1} s^{-1}$. Figure 3a shows the current–voltage

Table 2. Field-effect mobilities, on/off ratios, and threshold voltages of BBFBB, DHFBF, and DHFBBF transistors prepared at different substrate temperatures (T_D) on SiO$_2$ using top-contact geometry. The mobility values are an average of at least five devices. The standard deviation (SD) of all mobility values is also reported.

Oligomer	T_D [°C]	μ [cm^{2}V^{-1}s^{-1}] (SD)	On/off ratios	V_t [V]
BBFBB	25	0.012 (0.003)	2×10^6	–40
	50	0.06 (0.018)	2×10^6	–43
	100	4×10^{-4} (0.0001)	6×10^4	–31
DHFBF	25	6×10^{-4} (0.0004)	8×10^4	–46
	50	2×10^{-3} (0.0001)	1×10^4	–60
	80	3×10^{-3} (0.0016)	3×10^3	–52
	125	0.014 (0.0003)	6×10^6	–50
	150	2×10^{-3} (0.0008)	4×10^3	–65
DHFBBF	25	0.07 (0.001)	8×10^6	–46
	50	0.32 (0.11)	7×10^7	–22
	80	0.29 (0.009)	3×10^7	–30
	150	0.13 (0.002)	5×10^6	–29

transfer characteristics at $V_{DS} = -100$ V (V_{DS} = drain–source voltage) for DHFBBF at $T_D = 50$/C. Further increasing the substrate temperature resulted in a decrease in mobility, as has been observed with several other oligomers, mostly due to worse connectivity between larger grains and/or cracks arising from a mismatch in the thermal expansion coefficient between the substrate and the organic semiconductor film.[9,16,18] Figure 3b shows the shelf-life stability of DHFBBF devices ($T_D = 150$ °C) that were stored under ambient conditions. The actual testing was performed inside a glove-box to eliminate humidity fluctuations. The mobility values ranged from 0.10–0.13 when repeatedly tested over a period of 100 days and counting. The on/off ratios for the same devices varied from 5×10^5 to 8×10^6. We did observe a decrease in mobility and on/off ratio when the humidity of the ambient was greater than 45 %, which is commonly observed for other organic semiconductors.[19,20] However, the device performance is completely reversible when the water is removed. The performance is also retained after the devices are submerged under water and then blown dry with a stream of nitrogen. The devices are also stable under pulsed plasma conditions,[21] the results of which will be published elsewhere. Further correlation between the ionization potential of the oligomers and the sensitivity to moisture is underway

We have also investigated the photostability of these fluorene–phenylene derivatives. In solution, the UV-vis spectrum of DHFBBF (left in a sealed quartz cuvette in air-saturated chloroform with exposure to ambient light) does not change with time when measured over a period of more than 7 days. For comparison, pentacene has a half-life in air-saturated chloroform of about 10 min.[22] UV-irradiation studies (365 and 254 nm, 0.16 A, 60 Hz) were also performed on DHFBBF deposited onto glass substrates (see Supporting Information). No changes were observed under irradiation with 365 nm light (for longer than 30 h) but when the substrates were irradiated with higher energy, 254 nm, light for between 3 and 5 h, we did observe some photo-oxidation of the fluorene units, which introduces keto defects and affects the stability of the devices. This has been observed with other fluorene oligomers.[23] The photostability is still greatly improved over other high-mobility oligomers.

In conclusion, fluorene–phenylene derivatives have been prepared and characterized. These materials possess high ionization potentials, which lead to improved chemical stability. Average mobility values as high as 0.32 cm^2 V^{-1} s^{-1} and on/off ratios of ca. 10^8 were observed at substrate deposition temperatures as low as 50 °C. The high mobilities at low deposition temperatures are crucial because they allow the use of any type of plastic substrate. Further correlations between the HOMO level and susceptibility to moisture are underway.

Experimental

The synthesis and characterization of all oligomers is provided in the Supporting Information. Each oligomer was purified by vacuum sublimation using a three-temperature-zone furnace (Lindberg/Blue Thermo Electron Corporation). The vacuum level during sublimation was 10^{-6} Torr (1 Torr ≈ 133.3 Pa) or less. Highly doped n-type (100) Si wafers (<0.004 Ω cm) were used as substrates for the devices. SiO$_2$

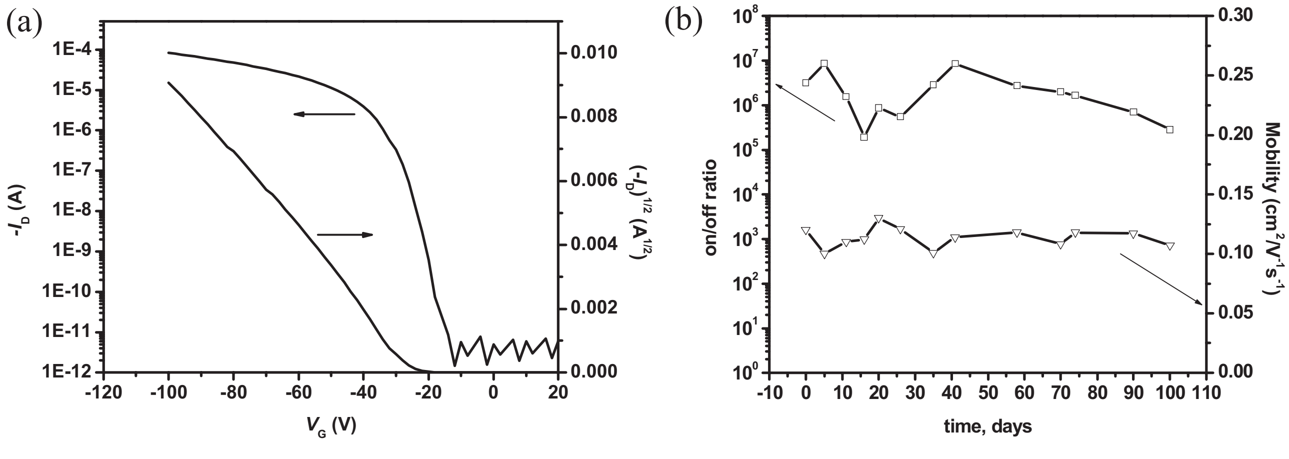

Figure 3. a) Transfer curve of DHFBBF at $T_D = 50$ °C. b) Field-effect mobility and on/off ratio for DHFBBF devices tested over a period of three months.

layers (unit area capacitance, C = 10 nF cm^{-2}), as gate dielectric, were thermally grown to 3000 Å thickness onto the Si substrates. The SiO_2/Si substrates were then cleaned with acetone and isopropyl alcohol. The wafers were then treated with octadecyl trimethoxysilane ($C_{18}H_{37}Si(OCH_3)_3$, OTS), which was grown from OTS vapor under reduced pressure and elevated temperature in a closed container.

40 nm organic films were vacuum-deposited onto the treated SiO_2/Si substrates at both room temperature and elevated temperatures, as denoted in the text, at a deposition rate of 1.0 Å s^{-1} and 10^{-6} Torr. The thin-film thickness of each derivative was determined in situ using a quartz-crystal microbalance (QCM).

A top-contact thin-film transistor was used for measuring the charge mobility of the fluorene–phenylene derivatives: gold source and drain electrodes (channel length (L) and width/length (W/L) of 200 µm and ca. 20 respectively) were vacuum-deposited through a shadow mask. The electrical characteristics of the organic field-effect transistors (OFET) devices were measured under accumulation mode using a Keithley 4200-SCS semiconductor parameter analyzer.

Atomic force microscopy (AFM) experiments were performed using a Multimode Nanoscope III (Digital Instruments/Veeco Metrology Group) using tapping mode. Out-of-plane X-ray diffraction (XRD) measurement was carried out with a Philips X'Pert PRO system. The beam wavelength was 1.5406 Å operated at 45 KeV and 40 mA. Electrochemical data was obtained by cyclic voltammetry in solution. The experiments were performed under argon in a saturated solution of anhydrous methylene chloride with 0.1 M tetrabutylammonium hexafluorophosphate as the supporting electrolyte. The scan rate was 50 mV s^{-1}. A silver wire was used as a pseudoreference electrode. All data in the text are referenced to the ferrocene/ferrocenium redox couple that was measured after the scan in the same system (Fc/Fc$^+$ $E_{1/2}$ = 0.598 V in our system).

Received: July 18, 2006
Revised: August 29, 2006

---

[1] C. Pannemann, T. Diekmann, U. Hilleringmann, *J. Mater. Res.* **2004**, *19*, 1999.
[2] C. Vaterlein, B. Ziegler, W. Gebauer, H. Neureiter, M. Stoldt, M. S. Weaver, P. Bauerle, M. Sokolowski, D. D. C. Bradley, E. Umbach, *Synth. Met.* **1996**, *76*, 133.
[3] Y. W. Wang, H. L. Cheng, Y K. Wang, T H. Hu, J. C. Ho, C. C. Lee, T. F. Lei, C. F. Yeh, *Thin Solid Films* **2004**, *467*, 215.
[4] T. Komoda, K. Kita, K. Kyuno, A. Toriumi, *Jpn. J. Appl. Phys., Part 1* **2003**, *42*, 3662.
[5] S. Ogawa, T. Naijo, Y. Kimura, H. Ishii, M. Niwano, *Appl. Phys. Lett.* **2005**, *86*, 252 104.
[6] C. R. Kagan, A. Afzali, T. O. Graham, *Appl. Phys. Lett.* **2005**, *86*, 193 505.
[7] H. Meng, Z. Bao, A. J. Lovinger, B. C. Wang, A. M. Mujsce, *J. Am. Chem. Soc.* **2001**, *123*, 9214.
[8] J. Locklin, D. W. Li, S. C. B. Mannsfeld, E. J. Borkent, H. Meng, R. Advincula, Z. Bao, *Chem. Mater.* **2005**, *17*, 3366.
[9] H. Meng, J. Zheng, A. J. Lovinger, B. C. Wang, P. G. Van Patten, Z. N. Bao, *Chem. Mater.* **2003**, *15*, 1778.
[10] H. Tian, J. Wang, J. Shi, D. Yan, L. Wang, Y. Geng, F. Wang, *J. Mater. Chem.* **2005**, *15*, 3026.
[11] N. Koch, A. Rajagopal, J. Ghijsen, R. L. Johnson, G. Leising, J. J. Pireaux, *J. Phys. Chem. B* **2000**, *104*, 1434.
[12] D. J. Gundlach, Y. Y. Lin, T. N. Jackson, D. G. Schlom, *Appl. Phys. Lett.* **1997**, *71*, 3853.
[13] H. Meng, F. Sun, M. B. Goldfinger, G. D. Jaycox, Z. Li, W. J. Marshall, G. S. Blackman, *J. Am. Chem. Soc.* **2005**, *127*, 2406.
[14] D. M. de Leeuw, M. M. J. Simenon, A R. Brown, R. E. F. Einerhand, *Synth. Met.* **1997**, *87*, 53.
[15] S. Verlaak, S. Steudel, P. Heremans, D. Janssen, M. S. Deleuze, *Phys. Rev. B* **2003**, *68*, 195 409.
[16] J. Locklin, M. Roberts, S. C. B. Mannsfeld, Z. Bao, *J.. Macromol. Sci., Polym. Rev.* **2006**, *46*, 79.
[17] R. Ruiz, D. Choudhary, B. Nickel, T. Toccoli, K. C. Chang, A. C. Mayer, P. Clancy, J. M. Blakely, R. L. Headrick, S. Iannotta, G. G. Malliaras, *Chem. Mater.* **2004**, *16*, 4497.
[18] Z. N. Bao, A. J. Lovinger, A. Dodabalapur, *Adv. Mater.* **1997**, *9*, 42.
[19] D. Li, E.-J. Borkent, R. Nortrup, H. Moon, H. Katz, Z. Bao, *Appl. Phys. Lett.* **2005**, *86*, 42 105.
[20] Z.-T. Zhu, J. T. Mason, R. Dieckmann, G. G. Malliaras, *Appl. Phys. Lett.* **2002**, *81*, 4643.
[21] M. T. van Os, B. Menges, R. Foerch, G. J. Vancso, W. Knoll, *Chem. Mater.* **1999**, *11*, 3252.
[22] A. Maliakal, K. Raghavachari, H. Katz, E. Chandross, T. Siegrist, *Chem. Mater.* **2004**, *16*, 4980.
[23] Y.-Y. Noh, D.-Y. Kim, Y. Yoshida, K. Yase, B.-J. Jung, E. Lim, H.-K. Shim, R. Azumi, *Appl. Phys. Lett.* **2004**, *85*, 2953.